# Experimental evidence of low-dimensional chaotic convection dynamics in a toroidal magnetized plasma

T. Živković and K. Rypdal
*Department of Physics and Technology, University of Tromsø, Norway*
(Received 23 January 2008; published 4 March 2008)

In a toroidal plasma confined by a purely toroidal magnetic field with a weak vertical field superimposed a system of convection cells are generated spontaneously, interacting with a background electron density gradient. The dynamics of this interaction is low-dimensional, chaotic, and consistent with solutions of the Lorenz equations in the diffusionless limit.

DOI: 10.1103/PhysRevE.77.037401 PACS number(s): 52.25.Xz, 52.35.Py, 52.25.Gj, 05.45.Ac

In geophysical fluids a major nondiffusive transport mechanism is the convection generated by the Rayleigh-Bénard (RB) instability, driven by a vertical temperature gradient in a fluid stratified by gravity [1]. Edward Lorenz presented a dynamical system in the form of an autonomous set of three coupled ordinary differential equations to describe the nonlinear evolution of this instability, and made the first systematic study of dissipative chaos [2]. The key control parameter in RB convection is the Rayleigh number, which depends proportionally on the imposed temperature gradient. Increasing this parameter the dynamics passes from a regime of stationary convection, via a regime of low-dimensional chaotic fluctuations of the amplitudes of the convection cells and the temperature profile, to a soft and hard turbulent regime (high-dimensional spatiotemporal chaos) [3].

It is well known that the RB instability has its counterpart in flute interchange instabilities in magnetized plasmas, driven unstable by pressure gradients in the direction of the radius of magnetic field curvature. In Ref. [4] this analogy was explored in detail by deriving the RB and the Lorenz models for a particular interchange instability, and discussing the similarities and differences in the underlying physics. In this Brief Report we demonstrate experimentally the creation of such a system of convection cells interacting with a background pressure gradient, and we show that the dynamics of this interaction is low-dimensional and consistent with solutions of the Lorenz equations in the so-called diffusionless limit.

An experimental setup suitable for a controlled study of convection cells generated by electrostatic flute interchange instabilities was presented in Ref. [5]. The experiments described in this Brief Report are performed in the same configuration; a hot filament cathode discharge in the "Blaamann" torus, which has major radius $R_0=65$ cm and minor radius $a=13$ cm, and helium gas pressure 0.35 Pa. The toroidal magnetic field is varied in the range $B=20-100$ mT, and a weak vertical magnetic field $B_z$ is superposed giving rise to helical magnetic field lines and a magnetic pitch ratio $r_B=|B_z|/B\sim 10^{-2}$.

In Ref. [5] the electron density and plasma potential profiles in a cross section of the plasma column were mapped. There is a vertically (in the $y$ direction) elongated "ridge" in the electron density, and a corresponding "valley" in the potential. The latter leads to a vertically downwards $\mathbf{E}\times\mathbf{B}$ drift of plasma on the outer low-field side of the torus and an upwards drift on the inner high-field side. The strength of the magnetic field $B$ was varied as a control parameter, keeping the pitch $r_B$ constant, and it was shown that flow surfaces, which were open in the lower part of the plasma column at small $B$, are gradually closing when $B$ increases. This closure gives rise to better confinement, and at a given threshold $B_T$ the density gradient in the radial ($x$) direction exceeds the excitation threshold of the flute interchange instability. It was further demonstrated that the resulting flute modes take the form of a helical coil elongated along the magnetic field, and thus that the vertical wavelength $\lambda$ corresponds to the distance a magnetic field line moves vertically when one turn is made in the toroidal direction. The mode can be considered as a helical convection roll frozen into the plasma, but since the plasma has a vertical drift the mode propagates at this drift velocity $v$, and a probe measuring the fluctuating electron pressure or plasma potential will observe a monochromatic signal on the Doppler-shifted frequency $f=v/\lambda$. Close to the instability threshold the plasma loss is still primarily along the open flow surfaces and there is no indication that the mode influences the background electron pressure profile. At higher $B$ the sharp spectral peak in the probe signal broadens, indicating fluctuations in the mode amplitude and/or phase, and in addition a low-frequency feature develops, which reflects fluctuations of the background profile. The closure of the flow surfaces also implies that the plasma now is transported across the field lines by anomalous mechanisms which involve the convection rolls and their interaction with the plasma pressure profile.

Figure 1 shows the power spectral density of the plasma potential fluctuations in different radial positions from the center of the plasma column ($x=8$ cm) and to the outer edge on the low-field side ($x=16$ cm). Similar spectra are obtained for the electron density fluctuations. A strong spectral hump around 20 kHz is observed in the radial interval $9<x<13$ cm, corresponding to the Doppler frequency of the propagating convection cells. This interval coincides with the steepest density slope where the local growth rate of the interchange instability has its maximum. The absence of this spectral peak outside this interval indicates the radial extent of the convection rolls. The spectra also have a low-frequency feature which is naturally ascribed to a more global fluctuation of the background density and potential profile. In the region where the convection rolls propagate there is a spectral peak around 2 kHz which is well separated from

 

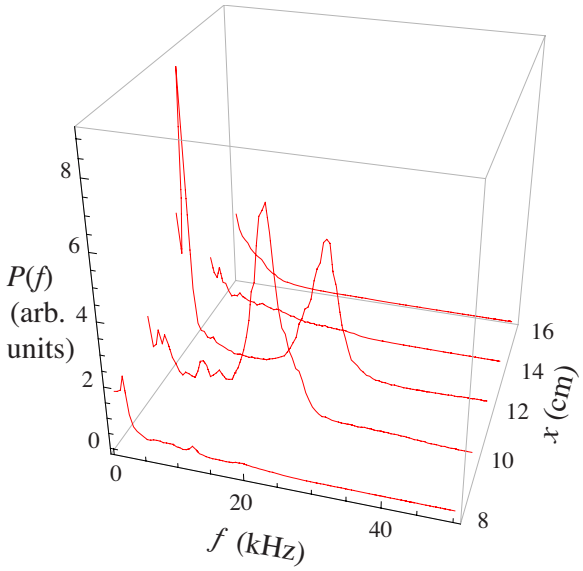


FIG. 1. (Color online) Power density spectra of plasma potential fluctuations in radial positions $x=8,10,12,14,16$ cm in the equatorial plane ($y=8$ cm) are shown in red (gray).

the hump around 20 kHz. This allows us to study separately the spatiotemporal structure of the high-frequency and the low-frequency dynamics.

We investigate the two-dimensional space-time evolution of the convection rolls in a cross section of the plasma column by a two-probe-system technique. The probe system is the same as described in Ref. [5], but in the present experiment one probe is kept fixed at a given position while the other probe is moved around the entire plasma column on a square grid $17\times17$ cm$^2$ with 1 cm spatial resolution. At every position of the moving probe simultaneous records are taken from both probe systems providing $10^5$ data points sampled at 100 kHz of electron pressure and plasma potential at the two positions. A standard conditional averaging technique [6] is then employed to map the average space-time evolution of the convection rolls in the cross section plane. A snapshot of the electron pressure perturbation is shown in the upper plot of Fig. 2(a). An animation shows that the structure propagates in the negative $y$ direction and the velocity corresponds to the $\mathbf{E}\times\mathbf{B}$ velocity estimated from the plasma potential profile. The radial extent of the electron pressure perturbation shows that the convection rolls are located on the outer electron density slope (on the low-field side of the density ridge), which is where the flute modes are unstable.

In order to study the fluctuations of the electron density profile we have to remove the influence of the propagating convection rolls from the signals. This is most easily done by low-pass filtering the signals via a moving average smoothing procedure to retain only the broad low-frequency hump in the spectrum. When the corresponding conditional averaging is performed on this filtered signal a standing-wave structure appears with wave vector directed radially (along $x$) as shown in Fig. 2(b). This structure encompasses only one wavelength in the radial direction and represents a more or less sinusoidal deformation of the pressure profile. The time

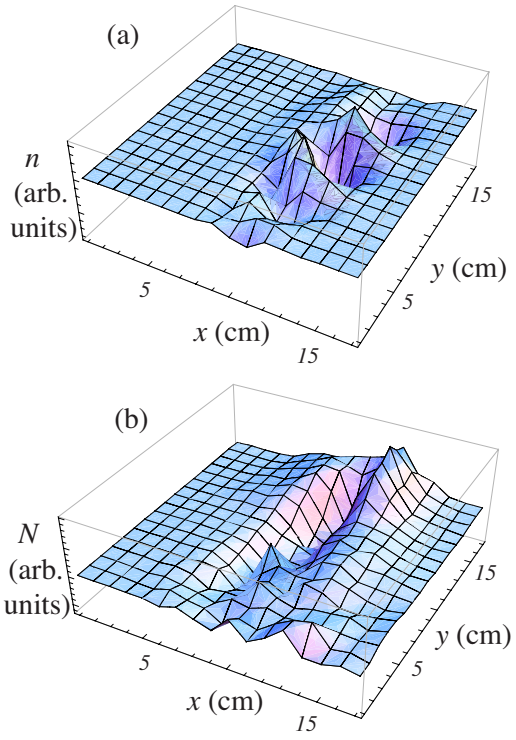


FIG. 2. (Color online) (a) Conditionally averaged electron density structures. Similar structures in plasma potential and animation of the time evolution of these structures [12] show that they are field aligned convection cells propagating with the vertical plasma flow in the negative $y$ direction. (b) Conditional average low-pass filtered density fluctuations. Animation of these low-frequency fluctuations show that they are standing oscillations of the plasma density profile [12].

evolution of the signal has an oscillatory character giving rise to the low-frequency peak in the power spectrum as shown in the trace for $x=12$ cm in Fig. 1. The oscillation, however, experiences sudden phase shifts which we will show are of chaotic nature. In the following we shall also argue that this signal is consistent with a chaotic solution of the Lorenz equations in the diffusionless limit [4]. These equations have the form

$$x' = -x - y,$$

$$y' = -zx,$$

$$z' = xy + R. \tag{1}$$

Unlike the full Lorenz equations, which have three free parameters, the diffusionless Lorenz equations have only one control parameter $R$. In Ref. [4] it was shown how $R$ depends on the physical parameters of the plasma experiment, but also that it in practice is very difficult to obtain even an order of magnitude estimate, since it depends on high powers of quantities which are difficult to measure with high accuracy. By applying a mean-field dimensional method [7] on the correlated low-pass filtered plasma potential and electron density fluctuations database, it was shown in Ref. [8] that the fluctuations in the present experiment show low-

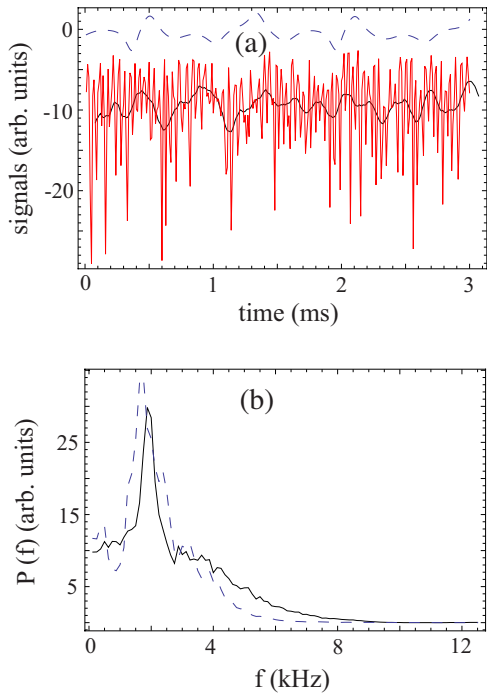


FIG. 3. (Color online) (a) Upper dashed trace is the signal for the profile gradient variable $z$ in the diffusionless Lorenz equations for $R=3.3$. The lower rapidly fluctuating red (gray) trace is the electron density fluctuation signal at $x=12$ cm, along with the black signal filtered by a moving average. (b) Spectral power density for diffusionless Lorenz signal (dashed) and for low-pass filtered electron density signal (black).

dimensional chaotic behavior, where the dynamics can be unfolded in the embedding dimension $D\sim 4$. This means that the diffusionless Lorenz equations might serve as a good model of the dynamics, but we need to find the appropriate value for $R$ from a qualitative investigation of the parameter space of solutions. There are of course an unlimited set of tests that can be employed to compare the dynamical features of the experimental signals and those generated from the model equations. Here we shall focus on a few which emphasize different qualities of the dynamics: power spectra, recurrence plots, and Lyapunov exponents.

A qualitative similar visual impression of the low-pass filtered experimental electron density signal and the corresponding model signal appears when we choose $R=3.3$, and the power spectral density for the two signals have similar structure [Fig. 3(b)].

This encourages us to test the low-pass filtered electron pressure signal specifically for chaotic properties and compare them with the solution of the diffusionless Lorenz equation. For this purpose we apply recurrence-plot analysis (see Refs. [9], [10]) which is a powerful tool for visualization of recurrence of phase-space trajectories. Prior to constructing a recurrence plot the phase space is reconstructed by time-delay embedding [11], where vectors $\mathbf{x}_i$ $(i=1,\ldots,T)$ are produced. Then a $T\times T$ matrix consisting of elements 0 and 1 is constructed. The matrix element $(i,j)$ is 1 if the distance is $\|\mathbf{x}_i-\mathbf{x}_j\|\leq r$ in the reconstructed phase space, and otherwise it is 0. The recurrence plot is simply a plot where the points

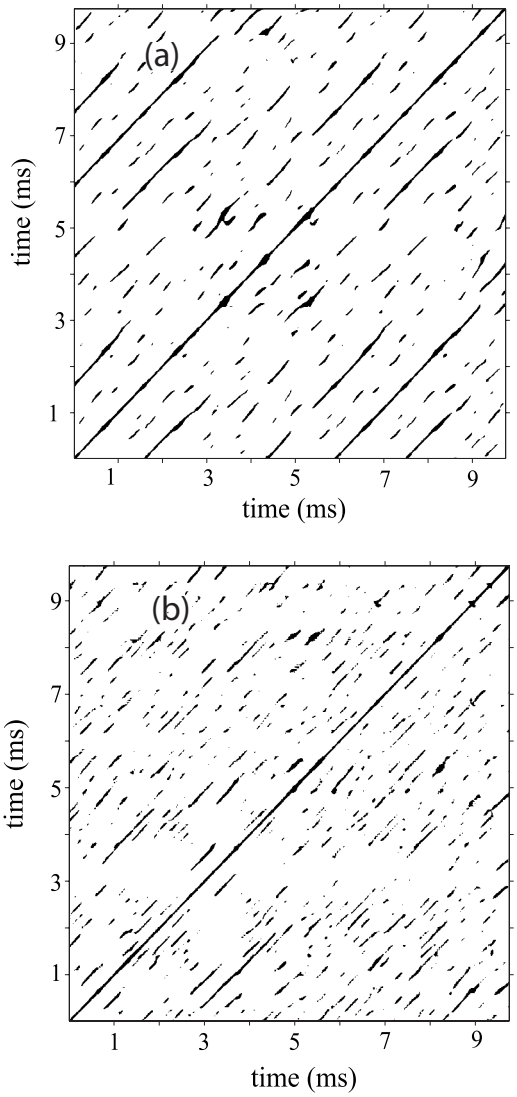


FIG. 4. Recurrence plots. (a) Low-pass filtered electron density fluctuations. (b) Diffusionless Lorenz equations.

$(i,j)$ for which the corresponding matrix element is 1 is marked by a dot.

The radius $r$ is fixed and chosen such that a sufficient number of points are found to reveal the fine structure of the plot. If the recurrence plot displays lines parallel to the main

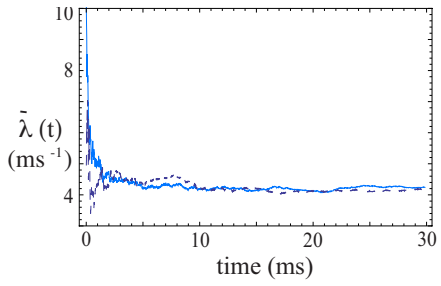


FIG. 5. (Color online) Computation of growth rate $\bar{\lambda}(t)$ from diffusionless Lorenz model signal (dashed) and low-pass filtered electron density signal in light blue (dark gray). The limit of large $t$ yields the Lyapunov exponent $\lambda$.

diagonal, recurrences of the trajectories in the phase space occur. If these lines are long and continuous the dynamics is periodic. Short diagonal lines indicate a chaotic state where trajectories recur for a short time and then diverge exponentially again. Recurrence plots for the time series of the low-pass filtered electron density fluctuations as well as for diffusionless Lorenz equation, shown in Fig. 4, have similar structure indicative of chaotic dynamics.

For chaotic signals the largest Lyapunov exponent is positive. We have computed this exponent for both signals by applying the same algorithm as described in Ref. [8]. Distances between pairs of points (fiducial point and its neighbor) are measured and compared after a fixed time. The logarithm of the ratio between these distances gives the current growth rate of divergence of the trajectories. We then follow the evolution of the pair of points and update the time-averaged growth rate $\bar{\lambda}(t)$ at each step by averaging over the previous steps during the time $t$. The Lyapunov exponent is estimated as the limit $\lambda=\lim_{t\to\infty}\bar{\lambda}(t)$. For the experimental data we compute the largest Lyapunov exponent for the reconstructed phase space with embedding dimension $D=4$ and time delay $\tau=5$. In Fig. 5 we plot $\bar{\lambda}(t)$ for the two signals. Both growth rates are positive and approach $\lambda \approx 4\ \mathrm{ms}^{-1}$. A Lyapunov exponent of this magnitude should give rise to a broadening of spectral peaks of the same order of magnitude, which is consistent with the spectra shown in Fig. 3.


[1] Lord Rayleigh, Philos. Mag. **32**, 529 (1916).
[2] E. N. Lorenz, J. Atmos. Sci. **20**, 130 (1963).
[3] F. Heslot, B. Castaing, and A. Libchaber, Phys. Rev. A **36**, 5870 (1987).
[4] K. Rypdal and O. Garcia, Phys. Plasmas **14**, 022101 (2007).
[5] K. Rypdal and S. Ratynskaia, Phys. Rev. Lett. **94**, 225002 (2005).
[6] F. J. Øynes, O.-M. Olsen, H. L. Pécseli, Å. Fredriksen, and K. Rypdal, Phys. Rev. E **57**, 2242 (1998).
[7] A. Y. Ukhorskiy, M. I. Sitnov, A. S. Sharma, and K. Papadopoulos, Ann. Geophysicae **21**, 1913 (2003).
[8] T. Zivkovic and K. Rypdal, e-print arXiv:0801.3151.
[9] J. P. Eckmann, S. O. Kamphorst, and D. Ruelle, Europhys. Lett. **4**, 973 (1987).
[10] N. Marwan, M. C. Romano, M. Thiel, and J. Kürths, Phys. Rep. **438**, 237 (2007).
[11] F. Takens, in *Dynamical Systems and Turbulence*, edited by D. Rand and L. S. Young (Springer, Berlin, 1981), p. 366.
[12] See EPAPS Document No. E-PLEEE8-77-105803 for the animation of conditionally averaged (a) electron density structures and (b) low-pass filtered electron density fluctuations. For more information on EPAPS, see http://www.aip.org/pubservs/epaps.html.